Biotechnology Reports 37 (2023) e00780

Contents lists available at ScienceDirect

Biotechnology Reports

journal homepage: www.elsevier.com/locate/btre

Research Article

Stable production of recombinant SARS-CoV-2 receptor-binding domain in mammalian cells with co-expression of a fluorescent reporter and its validation as antigenic target for COVID-19 serology testing

Jorge L. Arias-Arias [a,b], Silvia E. Molina-Castro [c], Laura Monturiol-Gross [d,*], Bruno Lomonte [d], Eugenia Corrales-Aguilar [a]

[a] Centro de Investigación en Enfermedades Tropicales (CIET), Facultad de Microbiología Universidad de Costa Rica, San José, 11501-2060, Costa Rica
[b] Dulbecco Lab Studio, Residencial Lisboa 2G, Alajuela, 20102, Costa Rica
[c] Instituto de Investigaciones en Salud (INISA), Universidad de Costa Rica, San José, 11501-2060, Costa Rica
[d] Instituto Clodomiro Picado (ICP), Facultad de Microbiología, Universidad de Costa Rica, San José, 11501-2060, Costa Rica

ARTICLE INFO

Keywords:
SARS-CoV-2
Recombinant RBD expression
Fluorescent protein
Mammalian cells
COVID-19 serology

ABSTRACT

SARS-CoV-2 receptor binding domain (RBD) recognizes the angiotensin converting enzyme 2 (ACE2) receptor in host cells that enables infection. Due to its antigenic specificity, RBD production is important for development of serological assays. Here we have established a system for stable RBD production in HEK 293T mammalian cells that simultaneously express the recombinant fluorescent protein dTomato, which enables kinetic monitoring of RBD expression by fluorescence microscopy. In addition, we have validated the use of this recombinant RBD in an ELISA assay for the detection of anti-RBD antibodies in serum samples of COVID-19 convalescent patients. Recombinant RBD generated using this approach can be useful for generation of antibody-based therapeutics against SARS-CoV-2, as well serological assays aimed to test antibody responses to this relevant virus.

1. Introduction

In December 2019, a pneumonia of unknown origin broke out in Wuhan, China [1,2 that rapidly spread throughout the world. The disease, named as coronavirus disease 2019 (COVID-19), is caused by SARS-CoV-2, a new member of the genus *Betacoronavirus* [3]. Extensive research and rapid worldwide collaboration helped characterization of the SARS-CoV-2 virus and enabled viral structure and viral protein functions to be defined [4,5,6]. Among these findings, the virion surface spike proteins were shown to mediate viral entry into host cells [7,8]. The spike protein consists of a S1 subunit responsible for receptor binding and a S2 subunit that mediates membrane fusion [9]. Since 2020, receptor recognition by SARS-CoV-2 has been widely studied. Similar to SARS-CoV-1, which caused a serious but limited epidemic in 2002–2003 [10], the spike protein of SARS-CoV-2 contains a receptor binding domain (RBD) on its S1 subunit (residues 319–541) that specifically recognizes the angiotensin converting enzyme 2 (ACE2), its receptor in host cells [11,7,9,12,10,13,14]. ACE2 is expressed in several human organs and tissues, including brain, kidney, cardiac muscle, respiratory endothelium and pneumocytes [11]. The crystal structure of the SARS-CoV-1 RBD showed that it contains a core and a receptor-binding motif (RBM) which mediates contact with ACE2 [10]. Compared to SARS-CoV-1, the major differences in the sequence of the spike protein of SARS-CoV-2 are three short insertions in the N-terminal domain as well as changes in four out of five of the key residues [1]. Structural features of the SARS-CoV-2 RBM, including an ACE2-binding ridge and hotspot-stabilizing residues, contribute to a higher ACE2-binding affinity when compared to SARS-CoV-1 RBM [13,14].

Considering that the RBD is the main viral structure for receptor binding, its recombinant and stable production is important for the development, testing and validation of intervention strategies against SARS-CoV-2 such as vaccines, neutralizing antibodies, and/or molecular inhibitors. SARS-CoV-2 RBD can be also used in serological assays, such as enzyme-linked immunosorbent assays (ELISA) [15] or surrogate neutralizing antibodies assays [16] that are of critical importance to help define previous exposure to SARS-CoV-2 or monitoring vaccine responses in populations. Strategies for recombinant production of RBD have been assessed using different expression systems such as *E. coli* [17], baculovirus-insect cells [15,16,18] mammalian cells [15,16,19,20, 21,22,23] yeast cells [19,24,25] and plants [21,26,27,28]. Mammalian

* Corresponding author.
E-mail address: laura.monturiol@ucr.ac.cr (L. Monturiol-Gross).

https://doi.org/10.1016/j.btre.2022.e00780
Received 29 September 2022; Received in revised form 8 December 2022; Accepted 30 December 2022
Available online 31 December 2022

cells have been shown to have higher yields of RBD expression than insect cells [15,29]. When compared with RBD produced in mammalian cells, production in *Komagataella phaffii* (*Pichia pastoris*) system yielded comparable amounts and similar structure and stability, but with marked differences in the glycosylation patterns [19]. RBD expression in mammalian cells has been achieved by both plasmid transient transfection [19,29,20,22] and human type 5 adenoviral transduction, the latter leading to around 7-fold higher levels of RBD protein in cell culture supernatants compared to transfected cultures [20]. Stable SARS-CoV-2 recombinant proteins expression in HEK 293T cells has been suggested and used [30,20,31], and stable transfection of SARS-CoV-2 RBD in CHO cells has been accomplished by others [23]. Altogether, given the importance of RBD as a highly specific antigen of SARS-CoV-2, its production by different approaches has been widely adopted for serological assays.

In the present work we have developed a system for stable RBD production in HEK 293T mammalian cells that simultaneously express the recombinant SARS-CoV-2 RBD and the orange fluorescent protein dTomato, enabling kinetic monitoring of RBD expression by fluorescence microscopy. Furthermore, we have validated the use of this recombinant RBD in an enzyme-linked immunoassay for the detection of human anti-RBD antibodies.

2. Materials and methods

2.1. Molecular design and cloning

The coding sequence of the SARS-CoV-2 RBD (Wuhan-Hu-1 isolate, GenBank: QHD43416.1, amino acids 319–541) with the spike signal peptide at the N-terminus and a C-terminal histidine tag (Amanat et al., 2020), was human codon optimized, commercially synthetized and cloned (GenScript, Piscataway, NJ, USA) into the NcoI and XbaI sites of the transposon-based vector pSBbi-RP (a gift from Eric Kowarz, Addgene plasmid #60,513) [32] to generate the plasmid pSBbi-RP-CoV2/RBD-Puro (Addgene plasmid #161,793). To increase the efficiency of translational initiation, a glycine was added at the second position of the signal peptide (MGFVFLVLLPLVSSQ) in order to introduce a codon that allowed the formation of a Kozak consensus sequence [33]. The functionality of the modified spike signal peptide was verified *in silico* using the online prediction method SignalP 5.0 (http://www.cbs.dtu.dk/services/SignalP/, likelihood value = 0.9859).

2.2. Stable cell line development

HEK 293T cells (ATCC, Manassas, VA, USA) were cultured in Dulbecco's modified Eagle medium (DMEM, Gibco, Gaithersburg, MD, USA) supplemented with 10% FBS, 1X GlutaMAX (Gibco), 1 mM sodium pyruvate, and 1X antibiotic-antimycotic solution, at 37 °C in an atmosphere of 5% CO_2. Stable HEK 293T/RBD cell line was established by double transfection with Lipofectamine 3000 (Invitrogen, Carlsbad, CA, USA) of the plasmid pSBbi-RP-CoV2/RBD-Puro (Addgene plasmid #161,793) and the vector pCMV(CAT)T7-SB100 codifying for the SB100X transposase (a gift from Zsuzsanna Izsvak, Addgene plasmid #34,879) [34]. At 72 h post-transfection, cells were selected during 2 days with 2 μg/ml of puromycin (Sigma, St. Louis, MO, USA) in DMEM 10% FBS. The selected stable cell line was grown and maintained in DMEM 10% FBS containing 0.25 μg/ml puromycin.

2.3. Live-cell imaging and Western Blot

HEK 293T/RBD cells stably expressing the fluorescent protein dTomato and the SARS-CoV-2 recombinant RBD were seeded in 6-well plates (Greiner Bio-One, Monroe, NC, USA) at a density of 5×10^5 cells/well in DMEM 10% FBS and incubated overnight at 37 °C/5% CO_2. Then, culture media was replaced with 2.5 ml/well of DMEM 2% FBS and cells were incubated for 96 h at 37 °C/5% CO_2. Cell images were acquired at 24, 48, 72 and 96 h with a Lionheart FX automated fluorescence microscope (BioTek, Winooski, VT, USA) using the 4X objective and the RFP filter/LED cube. Cell image analysis was performed with the software CellProfiler 4.0 (http://www.cellprofiler.org; Broad Institute, Cambridge, MA, USA). At the above-mentioned times, culture media samples were taken and stored at −20 °C. Later, samples were run on an SDS-PAGE gel, transferred to a PVDF membrane (Millipore, Burlington, MA, USA), stained with Ponceau S and blotted overnight at 4 °C with a 1:1000 dilution of mouse monoclonal anti-6x-His-tag antibody (Invitrogen, MA1–21,315). Finally, the membrane was treated for 1 h at room temperature with a 1:1000 dilution of goat polyclonal anti-mouse IgG HRP-conjugated antibody (Invitrogen, G-21,040) and visualized using the Super Signal West Pico Plus chemiluminescent substrate (Thermo, Waltham, MA, USA). Gel images were acquired with a ChemiDoc Imaging System (Bio-Rad, Hercules, CA, USA) and band analysis was performed with the software ImageLab 6.1 (Bio-Rad).

2.4. Recombinant proteins production and purification

HEK 293T/RBD were seeded in T75 flasks (Greiner Bio-One) at a density of 14×10^6 cells/flask in DMEM 10% FBS and incubated overnight at 37 °C/5% CO_2. Next morning, culture media was changed for 10 ml per flask of DMEM 2% FBS and cells were incubated for 96 h at 37 °C/5% CO_2. Supernatants were clarified by centrifugation at 2000 x *g* for 5 min and the recombinant proteins were purified using Ni^{2+}-affinity chromatography with a 5 ml HiTrap Chelating HP column (GE Healthcare, Chicago, IL, USA). The column was equilibrated and washed with a pH 8.0 buffer composed of 300 mM NaCl, 50 mM NaH_2PO_4, 10 mM or 50 mM imidazole, respectively. Proteins were eluted using a similar buffer with 250 mM imidazole. Finally, the buffer was exchanged for PBS pH 7.4 using Amicon 10 K ultrafiltration units (Millipore), sodium azide at 0.01% v/v was added and purified proteins were stored at 4 °C. Protein quantification was performed spectrophotometrically with the DC Protein Assay (Bio-Rad) in a Synergy HTX plate reader (BioTek) using bovine serum albumin (BSA) standards.

2.5. Mass spectrometry

SDS-PAGE protein bands of recombinant RBD were excised from gels and subjected to reduction (10 mM dithiothreitol), alkylation (50 mM iodoacetamide), and overnight in-gel digestion with sequencing grade bovine trypsin (in 25 mM ammonium bicarbonate) using an automated workstation (Intavis, Tübingen, Germany). The resulting peptides were submitted to nano-ESI-MS/MS on a Q-Exactive Plus™ mass spectrometer (Thermo). Briefly, 10 μL of each tryptic digest were loaded on an Acclaim™ PepMap™ C18 trap column (75 μm x 2 cm, 3 μm particle; Thermo), washed with 0.1% formic acid (solution A), and separated at 200 nl/min with an Easy-Spray™ C18 analytical column (75 μm x 15 cm, 3 μm particle; Thermo) using an EASY-nLC™ 1200 chromatograph (Thermo). A gradient from 0.1% formic acid (solution A) to 80% acetonitrile with 0.1% formic acid (solution B) was developed: 1–5% B in 1 min, 5–26% B in 25 min, 26–79% B in 4 min, 79–99% B in 1 min, and 99% B in 4 min, for a total time of 35 min. MS spectra were acquired in positive mode at 2.0 kV, with a capillary temperature of 200 °C, using 1 microscan at 400–1600 *m/z*, maximum injection time of 100 msec, AGC target of 3×10^6, and orbitrap resolution of 70,000. The top 10 ions with 2–5 positive charges were fragmented with AGC target of 1×10^5, maximum injection time of 110 msec, resolution 17,500, loop count 10, isolation window of 1.4 *m/z*, and a dynamic exclusion time of 5 s [35]. Resulting MS/MS spectra were processed for assignment of peptide matches against the amino acid sequence of the recombinant RBD using the software Peaks Studio Xpro (Bioinformatics Solutions, Waterloo, Canada). Cysteine carbamidomethylation was set as a fixed modification, while methionine oxidation and asparagine or glutamine deamidation were set as variable modifications, allowing up to 3 missed cleavages by trypsin. Parameters for match acceptance were set to

FDR<1% and −10lgP scores ≥50.

2.6. ELISA

The ELISA protocol was adapted from Amanat et al. 2020 [15]. 96-well plates (MaxiSorp F, NUNC, Thermo) were coated overnight at 4 °C with 50 µl per well of a 2–3 µg/ml solution of each respective RBD dissolved in 1X PBS (Gibco). Then, the coating solution was removed and 100 µl/well of 10% non-fat milk prepared in 1X PBS and 0.1% Tween 20 (PBST) was added to the plates at room temperature for 1 h as a blocking solution. Serum samples were inactivated at 56 °C for 30 min in order to reduce risk from any potential residual virus in the serum. A 1:50 dilution of serum was prepared in 1% non-fat milk prepared in PBST. The blocking solution was removed and 50 µl of each diluted serum was added to the plates for overnight incubation at 4 °C. Then, plates were washed three times with 100 µl/well of 0.1% PBST. Next, a 1:50.000 dilution of goat anti-human IgG–horseradish peroxidase (HRP) conjugated secondary antibody (Sigma, A0293) was prepared in 0.1% PBST and 50 µl/well of this secondary antibody was added for 30 min at room temperature. Plates were washed again three times with 0.1% PBST, followed by 50 µl/well of TMB (Sigma, T5525) dissolved in TMB Buffer (Na_2HPO_4 0.2 M and citric acid 0.1 M, pH 5.0, plus H_2O_2). This substrate was incubated on the plates for 10 min at room temperature and in the dark. Then the reaction was stopped by addition of 50 µl/well of H_2SO_4 1 M. The absorbance at 450 nm, with reference to 630 nm) was measured using an Epoch plate reader (BioTek). A prepandemic negative pool (20 human samples) and a SARS-CoV-2 reactive human monoclonal antibody CR3022 [36] were used as negative and positive controls, respectively. In this ELISA, a serum was determined as positive, if its A450 nm exceeded the A450nm obtained for the serum pool of pre-pandemic donors plus ten standard deviations (cutoff). Finally, cutoffs with the RBD stable and the transient RBD from [15] were compared.

2.7. Serum samples and ethics statement

Sera of SARS-CoV-2 positive patients were obtained after approval of the Ethical Board of the University of Costa Rica (CEC-164–2021). A cohort of 20 samples was randomly selected for the ELISA functional validation of the SARS-CoV-2 recombinant RBD produced in stable HEK 293T/RBD. Sera of 20 anonymous pre-pandemic serum donors stored in the lab from previous projects (CEC-VI-3970–2013) were used as a SARS-CoV-2 negative pool for setting the cutoff.

2.8. Statistics

Data are expressed as mean ± standard deviation (SD) of three independent experiments. Statistical significance of the differences between mean values was determined by using a one-way ANOVA followed by a Tukey's post hoc test with the software GraphPad Prism 8 (GraphPad Software, Inc, San Diego, CA, USA). The level of significance is denoted in the figures where statistics was applied.

3. Results

3.1. Stable production of recombinant RBD in HEK 293T cells can be monitored by the fluorescence of the co-expressed dTomato protein

RBD production was monitored in culture supernatants of stable HEK 293T/RBD cells by Western Blot (Fig. 1) with bands detected at a position corresponding to a molecular weight of 36 kDa, as expected [22, 23]. BSA stained with Ponceau Red was used as internal loading control of cell supernatant. Production of recombinant RBD in the culture supernatants was increased in a time-dependent manner when cultured with either 2% or 10% FBS media (Fig. 1b). The change was less patent in the 10% FBS conditions where the production plateaued at 72 h and the higher production occurred in the 2% FBS at 96 h, as qualitatively denoted by the formation of wider bands in the blots. As expected, there was no RBD in the supernatant samples from non-transfected control cells. The 2% FBS condition was chosen for further experiments. When the fluorescent intensity due to the dTomato expression was observed by live-cell imaging, it behaved similar to the RBD expression, that is, increased with time and reached the highest level at 96 h (Fig. 1c). No fluorescence was observed in the control cells even after 96 h of culture. When the dTomato fluorescence level was compared to the RBD band intensity, a similar trend in the increase was found (Fig. 1d), corroborating the qualitative differences observed with each technique. Statistically significant differences were found, in both cases, between the 24 h and the 96 h time points.

3.2. Stably produced recombinant RBD was successfully purified, and its identity was confirmed by tandem mass spectrometry

Recombinant RBD from 96 h supernatants of stable HEK 293T/RBD cells with 2% FBS culture medium was successfully purified and concentrated by Ni^{2+}-affinity chromatography and ultrafiltrated for buffer exchange. Fig. 2 shows the complete removal of the BSA and other unidentified bands from the ultrafiltrate (UF), that were present in the culture supernatant before (Pre) and after (Post) its passage through the purification column. The band corresponding to RBD had a greater intensity in the UF than in the Pre lane, indicating not only purification but also concentration of the recombinant protein. The RBD band was not detectable in the Post lane, indicating a total recovery of the RBD from the culture supernatant. Our yield for recombinant RBD produced in stable HEK 293T cells was 80–100 µg/ml, as calculated from three independent productions. The identity of the recombinant RBD protein was confirmed by in-gel tryptic digestion of electrophoretic bands, followed by tandem mass spectrometry. The resulting peptides matched the expected plasmid-encoded protein with a sequence coverage of 86%, as shown in Figure S2.

3.3. Stably produced recombinant RBD was antigenically functional for the detection of anti-RBD antibodies in serum samples from COVID-19 convalescent patients

The purified recombinant RBD produced in stable HEK 293T/RBD cells was used as antigen for the application of an in-house serological ELISA test and proved adequate for the detection of anti-RBD specific IgG antibodies in serum samples from COVID-19-recovered subjects. When compared with the recombinant RBD produced by transient transfection of HEK 293T cells following the protocol of Amanat et al. 2020 [15], the obtained values were generally lower and the difference between the results in both assays varied from sample to sample. However, in both cases, the method allowed a good discrimination between positive and negative results. The values for the negative controls showed the smallest variation between both assays (Fig. 3).

4. Discussion

Stable and constant production of SARS-CoV-2 RBD is relevant for the development of robust serological assays to test for antibodies against this virus in both ELISA or surrogate neutralization assays. With a still ongoing COVID-19 pandemic, it continues to be crucial to develop affordable and efficient serological tests for the evaluation of seroprevalence and vaccination efficacy. Initially, serological assays such as chemiluminescent immunoassay used either nucleocapsid protein (N), whole spike protein, S1 subunit, or peptides from the spike protein as a bait [37,38] but the use of RBD as a target in ELISAs has proved to be more specific towards SARS-CoV-2 [39]. Accordingly, in a surrogate neutralization assay, a dose-dependent specific binding between hACE2 and the RBD or S1, but not the N protein was reported, with the RBD producing the best binding characteristics [16]. Given the high

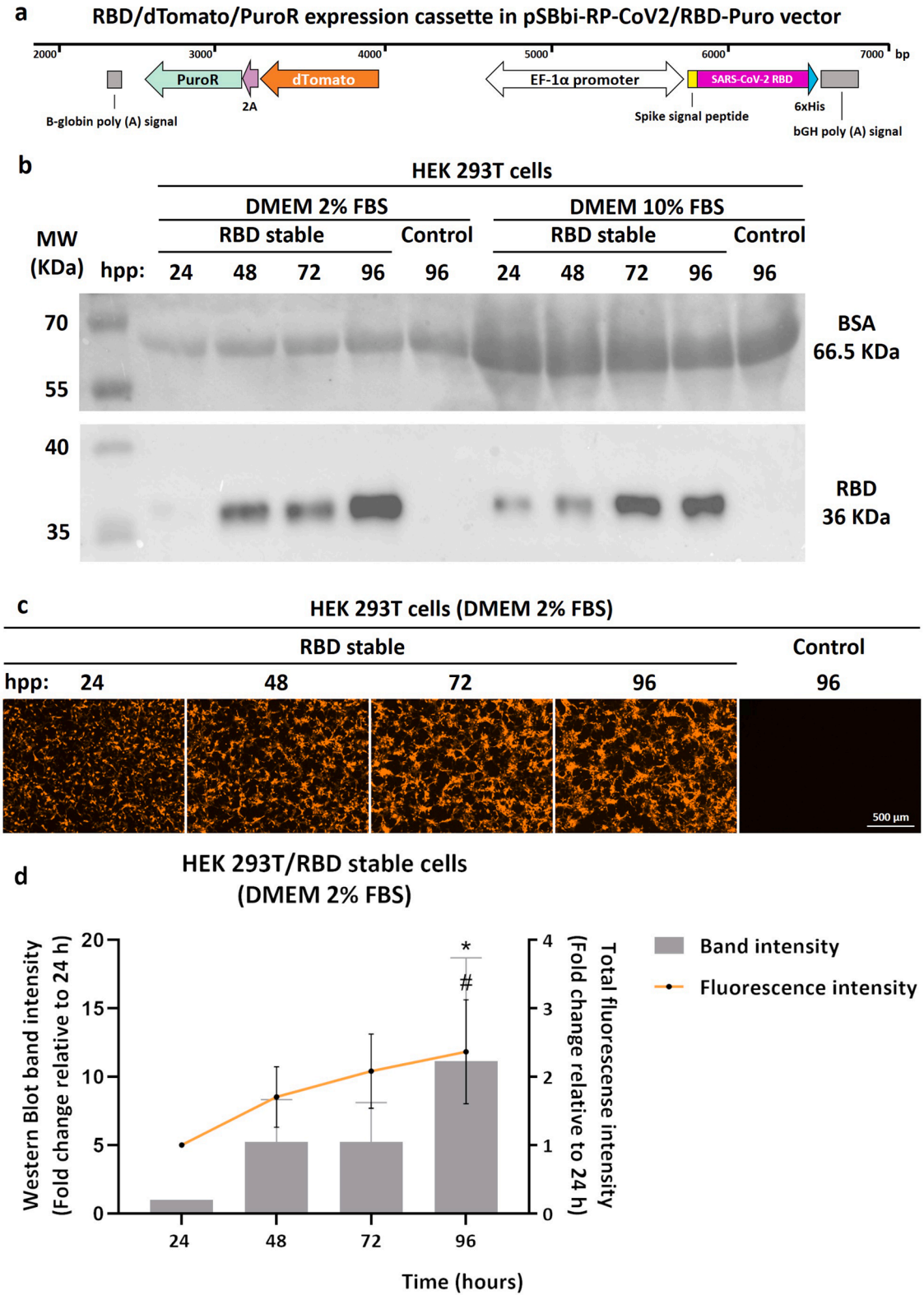

Fig. 1. Production kinetics of SARS-CoV-2 recombinant RBD and dTomato in stable HEK 293T/RBD cells. (a) Schematic representation of the polycistronic cassette for simultaneous expression of RBD, dTomato and puromycin-resistance gene (PuroR). The approximate location of each component into the pSBbi-RP-CoV2/RBD-Puro vector is depicted in base pair (bp). (b) Western Blot kinetic analysis of RBD in supernatants of wild-type HEK 293T (control) and stable HEK 293T/RBD cells incubated with culture media containing different percentages of fetal bovine serum (FBS). Ponceau S staining of the bovine serum albumin (BSA) from the culture media was used as a loading control for the SDS-PAGE. Representative cropped images from three independent experiments are shown (c) Fluorescence live-cell imaging kinetic analysis of dTomato expression into wild-type HEK 293T (control) and stable HEK 293T/RBD cells incubated with 2% FBS culture media. Representative images from three independent experiments are shown. (d) Relative quantification of RBD (Western Blot band intensity) and dTomato (Total fluorescence intensity) produced upon time in stable HEK 293T/RBD cells incubated with 2% FBS culture media. $*p = 0.0133$ compared with the Western Blot band intensity at 24 h. $\#p = 0.0201$ compared with the fluorescence intensity at 24 h. Data are expressed as means ± SD of three independent experiments.

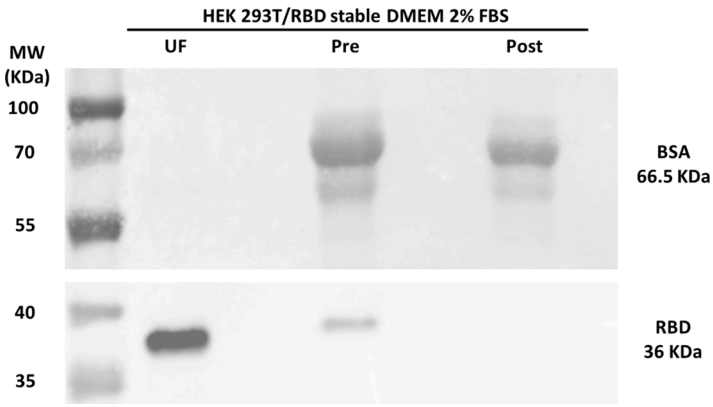

Fig. 2. Western Blot analysis of purified SARS-CoV-2 recombinant RBD produced in stable HEK 293T/RBD cells. The recombinant RBD present in supernatants of HEK 293T/RBD cells cultured for 96 h in DMEM 2% FBS was purified by Ni^{2+}-affinity chromatography and ultrafiltrated for buffer exchange. Samples from cells supernatants before (Pre) and after (Post) passage thought the purification column, as well as from the purified and ultrafiltrated recombinant RBD (UF), were analyzed by Western Blot using an anti-His-tag antibody. Ponceau S staining of BSA from the culture media was used as a visual indicator of purification efficiency. Representative cropped images from three independent experiments are shown.

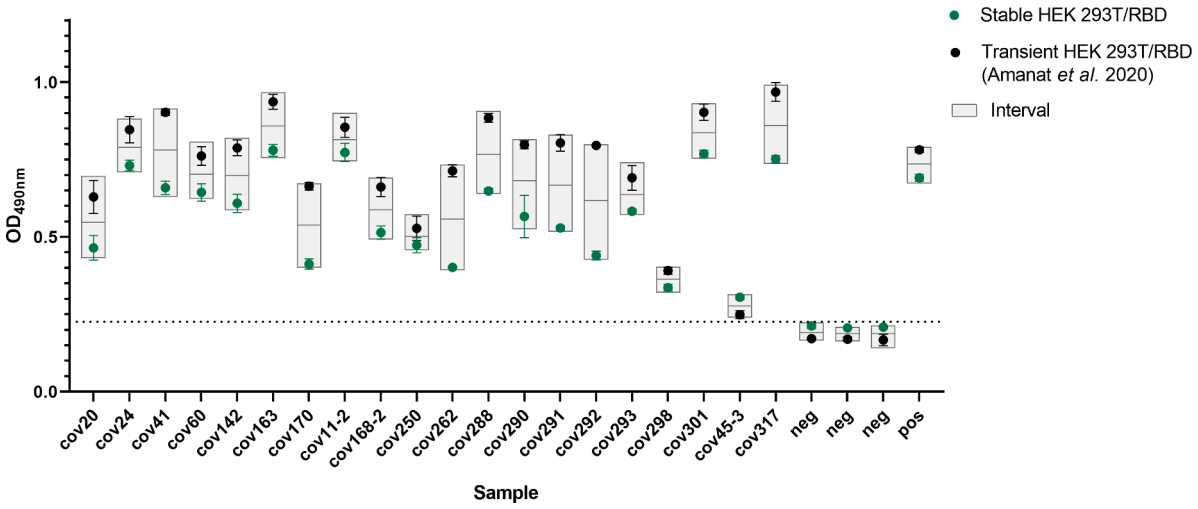

Fig. 3. Functional validation of SARS-CoV-2 recombinant RBD produced in stable HEK 293T/RBD cells as antigen for COVID-19 serology testing by ELISA. 20 Serum samples were detected in parallel in an ELISA, coating the plate with 3 ug/ml of purified RBD supernatants obtained from transiently transfected HEK 293T cells following Amanat et al. 2020 protocol (black circles) and from the stable HEK 293T/RBD cells (green circles). A cut-off was established by adding 10 standard deviations to the median OD490nm obtained for the negative pool (punctuated line). An interval between the two OD490nm obtained is highlighted in light gray. Data from three independent experiments is shown.

specificity of RBD for SARS-CoV-2 serology testing, the present report aimed to produce a recombinant RBD for forthcoming research and different biological applications.

We have developed a system for stable RBD production in mammalian cells that simultaneously express recombinant SARS-CoV-2 RBD and the fluorescent protein dTomato. We validated our system in HEK 293T cells due to the fact of being a cell line of human origin widely used for recombinant protein expression. However, we also used VeroE6 cells to prove the robustness of our genetic construct to successfully drive the expression and secretion of RBD, as those cells are widely used for coronavirus studies (Fig. S1). RBD production has been accomplished by several other groups [15,16,19,20,23,24,29,40] and diagnostic industries [39]. Furthermore, vectors for RBD expression are also commercially available. Although most approaches use transient transfection to produce the recombinant protein, it has been shown that RBD expression in HEK 293FS by adenoviral-mediated transduction leads to higher yields than the levels obtained after plasmid transient transfection [20]. Our approach generated stable HEK 293T expression of RBD by a double transfection of a cytomegalovirus vector (pCMV(CAT) T7-SB100) coding for the SB100X transposase and the polycistronic cassette for simultaneous expression of RBD, dTomato and puromycin-resistance gene (plasmid pSBbi-RP-CoV2/RBD-Puro) (Fig. 1a). Therefore, by changing the RBD coding sequence in the plasmid pSBbi-RP-CoV2/RBD-Puro our system could be adapted to produce different RBD versions corresponding to the clinically relevant SARS-CoV-2 variants, as the currently dominant Omicron strain. The use of mammalian cells has shown a better expression of both RBD and Spike proteins of SARS-CoV-2 than insect cells [15]. One advantage of HEK 293T cells as expression system is related to the achievement of proper post-translational modifications, a feature which could have a potential influence in diverse applications when proteins are produced in non-human cell lines [20]. The use of other eukaryotic expression systems as yeast or plant cells, even if advantageous in costs and up-scaling, often requires additional elements or modifications in order to achieve adequate physicochemical characteristics and biological responses [17,24,25,26]. Our system allows stable expression of a minimally modified RBD, saving time and resources needed for the generation of the transfection grade DNA used by the transient expression approaches. This also reduces the variability in the yields achieved as specific cell clones could be selected and preserved for future productions. For this purpose, the co-expression of the fluorescent protein dTomato is advantageous, as it not only allows an easy monitoring of the transfection efficiency during the generation of the stable cell line but can also be used in the selection of specific high-yield clones by fluorescence-activated cell sorting (FACS). Furthermore, the detection of the fluorescence generated by the co-expressed protein dTomato could be also used as a surrogate for the monitoring of the RBD production. As shown in Fig. 1, dTomato fluorescence levels following time-course expression of RBD

had a similar increase trend to RBD band intensity determined by western blot, which confirms usefulness of such surrogate approach to monitor levels of RBD generation. This could be also implemented as a strategy for the standardization of upscaled production protocols by measuring the general dTomato fluorescence to correlate with RBD expression levels in bioreactors [41,42, 43].

Highest RBD production in HEK293T cells was achieved in a 2% FBS environment at 96 h post-transfection, as shown in Fig. 1b. Purified recombinant RBD from cell supernatant was achieved by Ni^{2+}-affinity chromatography followed by ultrafiltration (Fig. 2), with yields in the 80–100 μg/ml range. Similar high yields (~100 μg/ml) of recombinant RBD are achieved even when HEK293SFcells are grown in serum-free media [20]. For comparison, several previously reported yields of RBD production in different expression systems are summarized in Table 1. Another study recently reported stable high production of RBD in mammalian CHO DG44 cells yielding 30 mg per liter of cell flask supernatant [23]. Using mammalian cell lines has the advantage of allowing post-translational modifications such as glycosylation, when compared to other systems [19,20,23]. Identification of our recombinant RBD protein was confirmed by tandem mass spectrometry (Fig. S2). The peptide sequence FPNITNLCPFGEVFNATR (*m/z* 2038.99) was not detected, likely explained by the potential N-linked glycosylation of this peptide at positions N331 (NIT) and N343 (NAT) which hampers its detection by mass spectrometry, as the increase in the peptide's mass excludes it from the analysis range for fragmentations as reported by others [19]. The overall sequence coverage for the recombinant protein in this analysis was 86%, clearly showing that protein species present in the sample belongs to the RBD from SARS-CoV-2.

Once obtained, we tested the functionality of our purified recombinant RBD by using it as antigen in an in-house ELISA test for the detection of anti-RBD antibodies in serum samples from COVID-19 convalescent patients (Fig. 3). Although the obtained values were generally lower than another in-house ELISA assay that also uses as antigen a recombinant RBD produced by transient transfection of HEK 293T cells [15], both methods allowed a good discrimination between positive and negative samples. As both ELISA assays correlated at each sample level, differences among them could be explained by slight variations in protein quantification of the corresponding purified RBD. Serological assays based on SARS-CoV-2 Spike protein and its RBD, have good sensitivity and specificity [15],29,40]. The present recombinant RBD proves to be functional in an ELISA test and could be also be suitable for further studies of other serological assays, such as neutralizing antibodies detection.

Overall, in the present work we developed a stable HEK 293T cell line for SARS-CoV-2 RBD production that simultaneously expresses this recombinant RBD and the fluorescent protein dTomato, allowing kinetic monitoring of viral protein expression by fluorescence microscopy. Additionally, we have tested the capability of this recombinant RBD in an ELISA assay aimed to detect anti-RBD antibodies from serum samples of COVID19 convalescent patients. The purified RBD using this approach can be useful for generation of antibody-based therapeutics against SARS-CoV-2, such as passive or active immunization, as well as for the development of serological assays aimed to test antibody responses to this widespread relevant virus.

Table 1
Expression levels of SARS-CoV-2 RBD in different expression systems.

Expression System		Yields	References
Bacteria	*Escherichia coli*	2 μg/ml (RP-HPLC purification)	[17]
Yeast	*Komagataella phaffii* (*Pichia pastoris*)	10–13 μg/ml (Lab. scale) (1)	[19]
		45 μg/ml (Bioreactor)	
		30–40 μg/ml (Bioreactor)(1)	[24]
		~12 to ~20 μg/ml (2)	[25]
Plants	*Nicotiana benthamiana*	8 μg/g leaf fresh weight	[27]
		117 ± 41 μg/g to 63 ± 10 μg/g fresh leaves (2)	[28]
		10 μg/g	[21]
Insect cells	*Trichoplusia ni* derived BTI-*TN*-5B1–4 cells (High Five)	1.5 μg/ml (1)	[15]
	Trichoplusia ni (Tnms42)	0.2 μg/ml (1)	[21]
Mammalian cells	HEK293T	5 μg/ml (1)	[19]
	HEK293T	80–100 μg/ml (1)	This study
	HEK293–6E	40 μg/ml (1)	[21]
	HEK293-E6	~25 μg/ml (1)	[29]
	HEK293SF-Adenovirus transfection	28.4 (±4.5) to 131.7 ± 27.2 μg/ml (Lab. Scale) (3)	[20]
		101.7 μg/ml (Bioreactor)	
		129.8 μg/ml (Bioreactor) (1)	
	HEK293SF-Transient transfection	1.5 ± 0.23 μg/ml to 17.7 ± 5.1 μg/ml (Lab. scale) (3)	[20]
		17.8 μg/ml (Bioreactor)	
		152 μg/ml (Bioreactor) (1)	
	CHO-K1	0.7 μg/ml (1)	[21]
	CHO-S	0.8 μg/ml (1)	[21]
	CHO-DG44	50 μg/ml (1) (polyclonal cell population)	[23]
		3000–7000 μg/ml (1) (high productivity clone)	
	Expi293F	11.5 (± 3.8) to 78.3 μg/ml (4)	[22]
	Expi293F	25–50 μg/ml (1)	[15]
	Expi293F	90 μg/ml (1)	[29]

(1)After Ni-NTA/Cu^{+2}/IMAC Column Elution.
(2)According to different RBD variants.
(3)According to different culture conditions.
(4)According to different RBD constructs and processing.

Funding

This work was supported by Universidad de Costa Rica (Fondo de Estímulo C1015, Grant UCREA C0344), International Centre for Genetic Engineering and Biotechnology (ICGEB, grant C1509). The funders had no role in study design, data collection and analysis, decision to publish, or preparation of the manuscript.

CRediT authorship contribution statement

Jorge L. Arias-Arias: Funding acquisition, Conceptualization, Methodology, Formal analysis, Investigation, Visualization, Writing – review & editing. **Silvia E. Molina-Castro:** Methodology, Formal analysis, Investigation, Writing – review & editing. **Laura Monturiol-Gross:** Funding acquisition, Project administration, Conceptualization, Writing – original draft, Writing – review & editing. **Bruno Lomonte:** Methodology, Formal analysis, Investigation, Writing – review & editing. **Eugenia Corrales-Aguilar:** Funding acquisition, Conceptualization, Methodology, Project administration, Supervision, Writing – review & editing.

Declaration of Competing Interest

The authors declare that they have no known competing financial interests or personal relationships that could have appeared to influence the work reported in this paper.

Data availability

Data generated during this study is included in the published article.

Acknowledgments

The authors thank Danilo Solano-Quesada and Francisco Vega-Aguilar from Universidad de Costa Rica for their invaluable technical assistance. We also thank Esteban Chaves-Olarte from Universidad de Costa Rica for his support with critical resources for protein purification. Thanks are also due to RED CYTED BUDEPAV-AM 219RT0573.

Supplementary materials

Supplementary material associated with this article can be found, in the online version, at doi:10.1016/j.btre.2022.e00780.

References

[1] P. Zhou, X. Yang, Xian-guang Wang, B. Hu, L. Zhang, W. Zhang, H. Guo, R. Jiang, M. Liu, Y. Chen, X. Shen, Xi Wang, F. Zhan, Y. Wang, G. Xiao, Z. Shi, A pneumonia outbreak associated with a new coronavirus of probable bat origin, Nature 579 (2020) 270–273, https://doi.org/10.1038/s41586-020-2012-7.

[2] N. Zhu, D. Zhang, W. Wang, X. Li, B. Yang, J. Song, X. Zhao, B. Huang, W. Shi, R. Lu, P. Niu, F. Zhan, X. Ma, D. Wang, W. Xu, G. Wu, G.F. Gao, D. Phil, W. Tan, A novel coronavirus from patients with pneumonia in China, N. Engl. J. Med. 382 (2019) 727–733, https://doi.org/10.1056/NEJMoa2001017.

[3] A.E. Gorbalenya, S.C. Baker, R.S. Baric, R.J. de Groot, C. Drosten, A.A. Gulyaeva, B. L. Haagmans, C. Lauber, A.M. Leontovich, B.W. Neuman, D. Penzar, S. Perlman, L. L.M. Poon, D.V. Samborskiy, I.A. Sidorov, I. Sola, J. Ziebuhr, The species severe acute respiratory syndrome- related coronavirus: classifying 2019-nCoV and naming it SARS-CoV-2, Nat. Microbiol. 5 (2020) 536–544, https://doi.org/10.1038/s41564-020-0695-z.

[4] W.T. Harvey, A.M. Carabelli, B. Jackson, R.K. Gupta, E.C. Thomson, E.M. Harrison, C. Ludden, R. Reeve, A. Rambaut, S.J. Peacock, D.L. Robertson, SARS-CoV-2 variants, spike mutations and immune escape, Nat. Rev. Microbiol. (2021), https://doi.org/10.1038/s41579-021-00573-0.

[5] C.B. Jackson, M. Farzan, B. Chen, H. Choe, Mechanisms of SARS-CoV-2 entry into cells, Nat. Rev. Mol. Cell Biol. (2022), https://doi.org/10.1038/s41580-021-00418-x.

[6] A. Mittal, A. Khattri, V. Verma, Structural and antigenic variations in the spike protein of emerging SARS-CoV-2 variants, PLoS Pathog (2022), https://doi.org/10.1371/journal.ppat.1010260.

[7] M. Hoffmann, H. Kleine-Weber, S. Schroeder, N. Krüger, T. Herrler, S. Erichsen, T. S. Schiergens, G. Herrler, N.-.H. Wu, A. Nitsche, M.A. Müller, C. Drosten, S. Pöhlmann, SARS-CoV-2 cell entry depends on ACE2 and TMPRSS2 and is blocked by a clinically proven protease inhibitor, Cell 181 (2020) 271–280.

[8] A.C. Walls, Y. Park, M.A. Tortorici, A. Wall, A.T. Mcguire, D. Veesler, Structure, function, and antigenicity of the SARS- structure, function, and antigenicity of the SARS-CoV-2 spike glycoprotein, Cell 180 (2020) 281–292, https://doi.org/10.1016/j.cell.2020.02.058.

[9] Y. Huang, C. Yang, X. Xu, W. Xu, S. Liu, Structural and functional properties of SARS-CoV-2 spike protein : potential antivirus drug development for COVID-19, Acta Pharmacol. Sin 41 (2020) 1141–1149, https://doi.org/10.1038/s41401-020-0485-4.

[10] F. Li, W. Li, M. Farzan, S.C. Harrison, Structure of SARS coronavirus spike receptor-binding domain complexed with Receptor, Science (1979) 309 (2005) 1864–1869.

[11] A.M. Baig, A. Khaleeq, H. Syeda, Elucidation of cellular targets and exploitation of the receptor-binding domain of SARS-CoV-2 for vaccine and monoclonal antibody synthesis, J. Med. Virol. 92 (2020) 2792–2803, https://doi.org/10.1002/jmv.26212.

[12] J. Lan, J. Ge, J. Yu, S. Shan, H. Zhou, S. Fan, Q. Zhang, X. Shi, Q. Wang, L. Zhang, X. Wang, Structure of the SARS-CoV-2 spike receptor-binding domain bound to the ACE2 receptor, Nature 581 (2020) 215–220, https://doi.org/10.1038/s41586-020-2180-5.

[13] J. Shang, G. Ye, K. Shi, Y. Wan, C. Luo, H. Aihara, Q. Geng, A. Auerbach, F. Li, Structural basis of receptor recognition by SARS-CoV-2, Nature 581 (2020) 221–224, https://doi.org/10.1038/s41586-020-2179-y.

[14] W. Tai, L. He, X. Zhang, J. Pu, D. Voronin, S. Jiang, Y. Zhou, L. Du, Characterization of the receptor-binding domain (RBD) of 2019 novel coronavirus: implication for development of RBD protein as a viral attachment inhibitor and vaccine, Cell Mol. Immunol. 17 (2020) 613–620, https://doi.org/10.1038/s41423-020-0400-4.

[15] F. Amanat, D. Stadlbauer, S. Strohmeier, T.H.O. Nguyen, V. Chromikova, M. McMahon, K. Jiang, G.A. Arunkumar, D. Jurczyszak, J. Polanco, M. Bermudez-Gonzalez, G. Kleiner, T. Aydillo, L. Miorin, D.S. Fierer, L.A. Lugo, E.M. Kojic, J. Stoever, S.T.H. Liu, C. Cunningham-Rundles, P.L. Felgner, T. Moran, A. García-Sastre, D. Caplivski, A.C. Cheng, K. Kedzierska, O. Vapalahti, J.M. Hepojoki, V. Simon, F. Krammer, A serological assay to detect SARS-CoV-2 seroconversion in humans, Nat. Med. 26 (2020) 1033–1036, https://doi.org/10.1038/s41591-020-0913-5.

[16] C.W. Tan, W.N. Chia, X. Qin, P. Liu, M.I. Chen, C. Tiu, Z. Hu, V.C. Chen, B. E. Young, W.R. Sia, Y. Tan, R. Foo, Y. Yi, D.C. Lye, D.E. Anderson, L.-.F. Wang, A SARS-CoV-2 surrogate virus neutralization test based on antibody-mediated blockage of ACE2–spike protein – protein interaction, Nat. Biotechnol. 38 (2020) 1073–1078, https://doi.org/10.1038/s41587-020-0631-z.

[17] S. Brindha, Y. Kuroda, A multi-disulfide receptor-binding domain (RBD) of the SARS-CoV-2 spike protein expressed in E. coli using a SEP-tag produces antisera interacting with the mammalian cell expressed spike (S1) protein, Int. J. Mol. Sci. 23 (2022), https://doi.org/10.3390/ijms23031703.

[18] R. Salem, A.A. El-Kholy, F.R. Waly, D. Ayman, A. Sakr, M. Hussein, Generation and utility of a single-chain fragment variable monoclonal antibody platform against a baculovirus expressed recombinant receptor binding domain of SARS-CoV-2 spike protein, Mol. Immunol. 141 (2022) 287–296, https://doi.org/10.1016/j.molimm.2021.12.006.

[19] C.R. Arbeitman, G. Auge, M. Blaustein, L. Bredeston, E.S. Corapi, P.O. Craig, L. A. Cossio, L. Dain, C. D'Alessio, F. Elias, N.B. Fernández, Y.B. Gándola, J. Gasulla, N. Gorojovsky, G.E. Gudesblat, M.G. Herrera, L.I. Ibañez, T. Idrovo, M.I. Rando, L. Kamenetzky, A.D. Nadra, D.G. Noseda, C.H. Paván, M.F. Pavan, M.F. Pignataro, E. Roman, L.A.M. Ruberto, Natalia Rubinstein2, Structural and functional comparison of SARS CoV 2 spike receptor binding domain produced in Pichia pastoris and mammalian cells, Sci. Rep. 10 (2020) 21779, https://doi.org/10.1038/s41598-020-78711-6.

[20] O. Farnós, A. Venereo-Sánchez, X. Xu, C. Chan, S. Dash, H. Chaabane, J. Sauvageau, F. Brahimi, U. Saragovi, D. Leclerc, A.A. Kamen, Rapid high-yield production of functional sars-cov-2 receptor binding domain by viral and non-viral transient expression for pre-clinical evaluation, Vaccines (Basel) 8 (2020) 1–20, https://doi.org/10.3390/vaccines8040654.

[21] M. Klausberger, M. Duerkop, H. Haslacher, G. Wozniak-Knopp, M. Cserjan-Puschmann, T. Perkmann, N. Lingg, P.P. Aguilar, E. Laurent, J. de Vos, M. Hofner, B. Holzer, M. Stadler, G. Manhart, K. Vierlinger, M. Egger, L. Milchram, E. Gludovacz, N. Marx, C. Köppl, C. Tauer, J. Beck, D. Maresch, C. Grünwald-Gruber, F. Strobl, P. Satzer, G. Stadlmayr, U. Vavra, J. Huber, M. Wahrmann, F. Eskandary, M.K. Breyer, D. Sieghart, P. Quehenberger, G. Leitner, R. Strassl, A. E. Egger, C. Irsara, A. Griesmacher, G. Hoermann, G. Weiss, R. Bellmann-Weiler, J. Loeffler-Ragg, N. Borth, R. Strasser, A. Jungbauer, R. Hahn, J. Mairhofer, B. Hartmann, N.B. Binder, G. Striedner, L. Mach, A. Weinhäusel, B. Dieplinger, F. Grebien, W. Gerner, C.J. Binder, R. Grabherr, A comprehensive antigen production and characterisation study for easy-to-implement, specific and quantitative SARS-CoV-2 serotests, EBioMedicine 67 (2021), https://doi.org/10.1016/j.ebiom.2021.103348.

[22] J. Mehalko, M. Drew, K. Snead, J.P. Denson, V. Wall, T. Taylor, K. Sadtler, S. Messing, W. Gillette, D. Esposito, Improved production of SARS-CoV-2 spike receptor-binding domain (RBD) for serology assays, Protein Expr. Purif. 179 (2021), https://doi.org/10.1016/j.pep.2020.105802.

[23] M.v. Sinegubova, N.A. Orlova, S.v. Kovnir, L.K. Dayanova, I.I. Vorobiev, High-level expression of the monomeric SARS-CoV-2 S protein RBD 320-537 in stably transfected CHO cells by the EEF1A1-based plasmid vector, PLoS ONE 16 (2021), https://doi.org/10.1371/journal.pone.0242890.

[24] M. Limonta-Fernández, G. Chinea-Santiago, A.M. Martín-Dunn, D. Gonzalez-Roche, M. Bequet-Romero, G. Marquez-Perera, I. González-Moya, C. Canaan-Haden-Ayala, A. Cabrales-Rico, L.A. Espinosa-Rodríguez, Y. Ramos-Gómez, I. Andujar-Martínez, L.J. González-López, M.P. de la Iglesia, J. Zamora-Sanchez, O. Cruz-Sui, G. Lemos-Pérez, G. Cabrera-Herrera, J. Valdes-Hernández, E. Martinez-Diaz, E. Pimentel-Vazquez, M. Ayala-Avila, G. Guillén-Nieto, An engineered SARS-CoV-2 receptor-binding domain produced in Pichia pastoris as a candidate vaccine antigen, N. Biotechnol. 72 (2022) 11–21, https://doi.org/10.1016/j.nbt.2022.08.002.

[25] Neil C. Dalvie, Sergio A. Rodriguez-Aponte, Brittany L. Hartwell, Lisa H. Tostanoski, Andrew M. Biedermann, Laura E. Crowell, Kawaljit Kaur, Ozan S. Kumru, Lauren Carter, Jingyou Yu, Aiquan Chang, Katherine McMahan, Thomas Courant, Celia Lebas, Ashley A. Lemnios, Kristen A. Rodrigues, Murillo Silva, Ryan S. Johnston, Christopher A. Naranjo, Mary Kate Tracey, Joseph R. Brady, Charles A. Whittaker, Dongsoo Yun, Natalie Brunette, Jing Yang Wang, Carl Walkey, Brooke Fiala, Swagata Kar, Maciel Porto, Megan Lok, Hanne Andersen, Mark G. Lewis, Kerry R. Love, Danielle L. Camp, Judith Maxwell Silverman, Harry Kleanthous, Sangeeta B. Joshi, David B. Volkin, Patrice M. Dubois, Nicolas Collin, Neil P. King, Dan H. Barouch, Darrell J. Irvine, J. Christopher Love, Engineered SARS-CoV-2 receptor binding domain improves manufacturability in yeast and immunogenicity in mice, PNAS 118 (2021) 1–9, https://doi.org/10.1073/pnas.2106845118/-/DCSupplemental.

[26] J. König-Beihammer, U. Vavra, Y.J. Shin, C. Veit, C. Grünwald-Gruber, Y. Gillitschka, J. Huber, M. Hofner, K. Vierlinger, D. Mitteregger, A. Weinhäusel, R. Strasser, In planta production of the receptor-binding domain from SARS-CoV-2 with human blood group A glycan structures, Front. Chem. 9 (2022), https://doi.org/10.3389/fchem.2021.816544.

[27] K. Rattanapisit, B. Shanmugaraj, S. Manopwisedjaroen, P.B. Purwono, K. Siriwattananon, N. Khorattanakulchai, O. Hanittinan, W. Boonyayothin, A. Thitithanyanont, D.R. Smith, W. Phoolcharoen, Rapid production of SARS-CoV-2 receptor binding domain (RBD) and spike specific monoclonal antibody CR3022 in Nicotiana benthamiana, Sci. Rep. 10 (2020), https://doi.org/10.1038/s41598-020-74904-1.

[28] Y.-J. Shin, J. König-Beihammer, U. Vavra, J. Schwestka, N.F. Kienzl, M. Klausberger, E. Laurent, C. Grünwald-Gruber, K. Vierlinger, M. Hofner, E. Margolin, A. Weinhäusel, E. Stöger, L. Mach, R. Strasser, N-Glycosylation of the SARS-CoV-2 receptor binding domain is important for functional expression in plants, Front. Plant Sci. 12 (2021), https://doi.org/10.3389/fpls.2021.689104.

[29] R. Castro, L.S. Nobre, R.P. Eleutério, M. Thomaz, A. Pires, S.M. Monteiro, S. Mendes, R.A. Gomes, J.J. Clemente, M.F.Q. Sousa, F. Pinto, A.C. Silva, M. C. Freitas, A.R. Lemos, O. Akpogheneta, L. Kosack, M.L. Bergman, N. Duarte, P. Matoso, J. Costa, T.M. Bandeiras, P. Gomes-Alves, C.P. Gonçalves, J. Demengeot, P.M. Alves, Production of high-quality SARS-CoV-2 antigens: impact of bioprocess

and storage on glycosylation, biophysical attributes, and ELISA serologic tests performance, Biotechnol. Bioeng. 118 (2021) 2202–2219, https://doi.org/10.1002/bit.27725.

[30] D. Esposito, J. Mehalko, M. Drew, K. Snead, V. Wall, T. Taylor, P. Frank, J. P. Denson, M. Hong, G. Gulten, K. Sadtler, S. Messing, W. Gillette, Optimizing high-yield production of SARS-CoV-2 soluble spike trimers for serology assays, Protein Expr. Purif. 174 (2020), 105686, https://doi.org/10.1016/j.pep.2020.105686.

[31] O. Minenkova, D. Santapaola, F.M. Milazzo, A.M. Anastasi, G. Battistuzzi, C. Chiapparino, A. Rosi, G. Gritti, G. Borleri, A. Rambaldi, C. Dental, C. Viollet, B. Pagano, L. Salvini, E. Marra, L. Luberto, A. Rossi, A. Riccio, E. Merlo Pich, M. G. Santoro, R. de Santis, Human inhalable antibody fragments neutralizing SARS-CoV-2 variants for COVID-19 therapy, Mol. Therapy 30 (2022) 1979–1993, https://doi.org/10.1016/j.ymthe.2022.02.013.

[32] E. Kowarz, D. Löscher, R. Marschalek, Optimized Sleeping Beauty transposons rapidly generate stable transgenic cell lines, Biotechnol. J. 10 (2015) 647–653, https://doi.org/10.1002/biot.201400821.

[33] M. Kozak, Compilation and analysis of sequences upstream from the translational start site in eukaryotic mRNAs, Nucleic Acids Res. 12 (1984) 857–872, https://doi.org/10.1093/nar/12.2.857.

[34] L. Mátés, M.K.L. Chuah, E. Belay, B. Jerchow, N. Manoj, A. Acosta-Sanchez, D. P. Grzela, A. Schmitt, K. Becker, J. Matrai, L. Ma, E. Samara-Kuko, C. Gysemans, D. Pryputniewicz, C. Miskey, B. Fletcher, T. Vandendriessche, Z. Ivics, Z. Izsvák, Molecular evolution of a novel hyperactive Sleeping Beauty transposase enables robust stable gene transfer in vertebrates, Nat. Genet. 41 (2009) 753–761, https://doi.org/10.1038/ng.343.

[35] B. Lomonte, J. Fernández, Solving the microheterogeneity of Bothrops asper myotoxin-II by high-resolution mass spectrometry: insights into C-terminal region variability in Lys49-phospholipase A2 homologs, Toxicon 210 (2022) 123–131, https://doi.org/10.1016/j.toxicon.2022.02.024.

[36] J. ter Meulen, E.N. van den Brink, L.L.M. Poon, W.E. Marissen, C.S.W. Leung, F. Cox, C.Y. Cheung, A.Q. Bakker, J.A. Bogaards, E. van Deventer, W. Preiser, H. W. Doerr, V.T. Chow, J. de Kruif, J.S.M. Peiris, J. Goudsmit, Human monoclonal antibody combination against SARS coronavirus: synergy and coverage of escape mutants, PLoS Med. 3 (2006) 1071–1079, https://doi.org/10.1371/journal.pmed.0030237.

[37] Y. Jin, M. Wang, Z. Zuo, C. Fan, F. Ye, Z. Cai, Y. Wang, H. Cui, K. Pan, A. Xu, Diagnostic value and dynamic variance of serum antibody in coronavirus disease 2019, Int. J. Infect. Dis. 94 (2020) 49–52, https://doi.org/10.1016/j.ijid.2020.03.065.

[38] Q.X. Long, B.Z. Liu, H.J. Deng, G.C. Wu, K. Deng, Y.K. Chen, P. Liao, J.F. Qiu, Y. Lin, X.F. Cai, D.Q. Wang, Y. Hu, J.H. Ren, N. Tang, Y.Y. Xu, L.H. Yu, Z. Mo, F. Gong, X.L. Zhang, W.G. Tian, L. Hu, X.X. Zhang, J.L. Xiang, H.X. Du, H.W. Liu, C. H. Lang, X.H. Luo, S.B. Wu, X.P. Cui, Z. Zhou, M.M. Zhu, J. Wang, C.J. Xue, X.F. Li, L. Wang, Z.J. Li, K. Wang, C.C. Niu, Q.J. Yang, X.J. Tang, Y. Zhang, X.M. Liu, J. J. Li, D.C. Zhang, F. Zhang, P. Liu, J. Yuan, Q. Li, J.L. Hu, J. Chen, A.L. Huang, Antibody responses to SARS-CoV-2 in patients with COVID-19, Nat. Med. 26 (2020) 845–848, https://doi.org/10.1038/s41591-020-0897-1.

[39] R. Lassaunière, A. Frische, Z.B. Harboe, A.C.Y. Nielsen, A. Fomsgaard, K. A. Krogfelt, C.S. Jørgensen, Evaluation of Nine Commercial SARS-CoV-2 Immunoassays (2020) 1–15, https://doi.org/10.1101/2020.04.09.20056325, medRxiv Pre print.

[40] N. Okba, M. Muller, W. Li, C. Wang, C. GeurtsvanKessel, V. Corman, M. Lamers, R. Sikkema, E. de Bruin, F. Chandler, Y. Yazdanpanah, Q. le Hingrat, D. Descamps, N. Houhou-Fidouh, C. Reusken, B. Jan Bosc, C. Drosten, M. Koopmans, B. Haagmans, SARS-CoV-2 Antibody Responses in COVID-19 Patients, Emerg. Infect. Dis. 26 (2020) 1478–1488, https://doi.org/10.1101/2020.03.11.987958.

[41] T. Broger, R.P. Odermatt, P. Huber, B. Sonnleitner, Real-time on-line flow cytometry for bioprocess monitoring, J. Biotechnol. 154 (2011) 240–247, https://doi.org/10.1016/j.jbiotec.2011.05.003.

[42] N. von den Eichen, L. Bromig, V. Sidarava, H. Marienberg, D. Weuster-Botz, Automated multi-scale cascade of parallel stirred-tank bioreactors for fast protein expression studies, J. Biotechnol. 332 (2021) 103–113, https://doi.org/10.1016/j.jbiotec.2021.03.021.

[43] Zhao, R., Natarajan, A., Srienc, F., 1999. A Flow Injection Flow Cytometry System for On-Line Monitoring of Bioreactors.